Articles

Fabrication of Unique Porous Polyimide Nanoparticles Using a Reprecipitation Method

Gufan Zhao, Takayuki Ishizaka, Hitoshi Kasai, Hidetoshi Oikawa,* and Hachiro Nakanishi

Institute of Multidisciplinary Research for Advanced Materials, Tohoku University, Katahira 2-1-1, Aobaku, Sendai 980-8577, Japan

Received November 14, 2006. Revised Manuscript Received February 9, 2007

Porous polyimide (PI) nanoparticles were fabricated using the reprecipitation method, with a second polymer as a porogen, and subsequent imidization. Poly(acrylic acid) was a suitable porogen for generating unprecedented PI nanoparticles having superficial nanopores, the sizes of which were in the range 20−70 nm. The porous morphology of the PI nanoparticles was affected mainly by the molecular weight and content of poly(acrylic acid). After thermal imidization, almost no poly(acrylic acid) remained inside the porous PI nanoparticles. Infrared spectroscopy and thermogravimetric analysis indicated that the porous nanoparticles consisted purely of PI and exhibited high thermal stability (5% weight loss temperature: 400 °C). The porous structure probably resulted from microphase separation of poly(amic acid) and poly(acrylic acid) during the reprecipitation process. This strategy provides a new means for improving the degree of porosity of PI nanoparticles, which have the potential for application as alternative materials for preparing interlayer dielectrics.

Introduction

The processing speeds of microchips continue to increase as densities increase in the semiconductor industry. As a result of the remarkable increase in the number of interlayer dielectrics, wiring delays dominate the total signal delay in ultralarge-scale integrated circuits (ULSI). When the device size is decreased, the so-called resistance−capacitance (RC) delay and the crosstalk noise between metal interconnects offset any gain in chip performance. To avoid these undesirable phenomena, a replacement dielectric for silicon dioxide must be found. In addition, it is important that the interlayer dielectrics exhibit high thermal stability and low dielectric constants.[1,2] Polyimides (PIs) are among the most promising candidates for use as next-generation interlayer dielectrics because of their unique physicochemical properties, including excellent thermal stability, low relative permittivity, and good adhesion properties. Unfortunately, their dielectric constants (k) are ca. 2.4−3.0, even for fluorinated PIs, and hence, they fail the requirements of ultralow k materials ($k < 2.0$).

According to the Maxwell−Garnett model,[3] PI films with porous structures have substantially reduced dielectric constants (because the dielectric constant of air is unity). Porous PI films have been prepared through the pyrolysis of phase-separated polymers and/or polymer blends films.[4−6] Their pore sizes are readily controlled through modification of the polymer blend ratio. Hedrick et al. reported[7,8] some porous PI films exhibiting pore sizes on the nanoscale when employing block copolymers; they prepared porous PI films through pyrolysis of thermally labile polymers as the dispersed phase in the PI matrix. In particular, a so-called nanofoam was produced as a PI film possessing a low dielectric constant ($k = 2.56$).

An alternative approach to the preparation of porous PI films exhibiting higher voidages is the assembly of multilayered films of PI nanoparticles, i.e., system in which air voids are formed between the PI nanoparticles. Such PI nanoparticles can be prepared using the reprecipitation method and subsequent imidization.[9] The reprecipitation method is a convenient technique for fabricating organic and polymer nanoparticles and/or nanocrystals in a dispersion medium.[10−13] The sizes of the resulting PI nanoparticles exist

* To whom correspondence should be addressed. Phone: 81-22-217-6357. Fax: 81-22-217-5645. E-mail: oikawah@tagen.tohoku.ac.jp.

(1) Maier, G. *Prog. Polym. Sci.* **2001**, *26*, 3.
(2) *International Technology Roadmap for Semiconductors*; http://www.itrs.net (accessed Feb 2007).
(3) Garnett, J. C. M. *Philos. Trans. R. Soc. London, Ser. A* **1904**, *203*, 385.
(4) Takeichi, T.; Yamazaki, Y.; Ito, A.; Zuo, M. *J. Photopolym. Sci. Technol.* **1999**, *12*, 203.
(5) Takeichi, T.; Yamazaki, Y. *J. Photopolym. Sci. Technol.* **2000**, *13*, 333.
(6) Takeichi, T.; Yamazaki, Y.; Zuo, M.; Ito, A.; Matsumoto, A.; Inagaki, M. *Carbon* **2001**, *39*, 257.
(7) Hedrick, J. L.; Miller, R. D.; Hawker, C. J.; Carter, K. R.; Volksen, W.; Yoon, D. Y.; Trollsas, M. *Adv. Mater.* **1998**, *10*, 1049.
(8) Hedrick, J. L.; Russel, T. P.; Labadie, J. W.; Lucas, M.; Swanson, S. A. *Polymer* **1995**, *36*, 2685.
(9) Suzuki, M.; Kasai, H.; Miura, H.; Okada, S.; Nakanishi, H.; Oikawa, H.; Nihira, T.; Fukuro, H. *Mol. Cryst. Liq. Cryst.* **2003**, *406*, 151.
(10) Kasai, H.; Nalwa, H. S.; Oikawa, H.; Okada, S.; Matsuda, H.; Minami, N.; Kakuta, A.; Ono, K.; Mukoh, A.; Naknishi, H. *Jpn. J. Appl. Phys.* **1992**, *31*, L1132.

10.1021/cm062709w CCC: $37.00
Published on Web 03/27/2007

Scheme 1

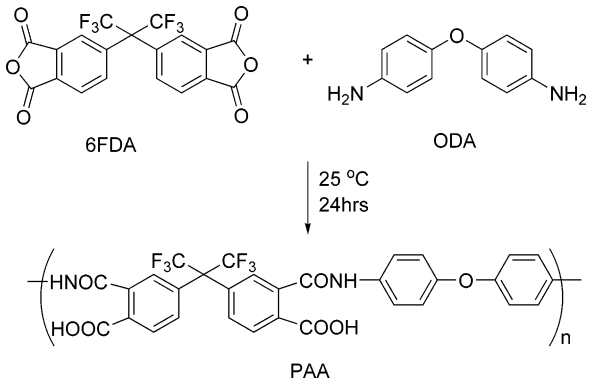

in the range from 50 to 500 nm. Multilayered films of the PI nanoparticles have been prepared using the electrophoretic deposition method;[14,15] these films exhibited dielectric constants below 2.5,[16] but still higher than 2.0. Thus, their porosity was not sufficiently high to fulfill future demand (i.e., $k < 2.0$).

On the other hand, polymer nanoparticles that display microphase-separated structures have received a significant amount of attention for their potential applications in biomedical and microelectronic fields. Shimomura et al. developed a simple method for preparing spherical block-copolymer nanoparticles through evaporation of the good solvent.[17] Okubo et al. reported the fabrication of golf-ball-like polymer particles through phase separation of polymers during seeded emulsion polymerizations.[18] To further improve such porosity, we focused on incorporating pores into each PI nanoparticle through microphase separation of polymers within the particles.

In this study, we employed a second polymer as the porogen to prepare porous PI nanoparticles through the reprecipitation method and then investigated how the porogen species and the reprecipitation conditions affected the porous structures of the resulting PI nanoparticles. Herein, we discuss in detail the formation process of the superficial nanopores.

Experimental Section

Poly(amic acid) (PAA), which had been synthesized (Scheme 1) from 4,4′-(hexafluoroisopropylidene)diphthalic anhydride (6FDA) and 4,4′-oxydianiline (ODA), was supplied by Nissan Chemical Industries. Poly(acrylic acid) (PAS1, $M_w = 2000$; PAS2, $M_v = 450\,000$; Aldrich) and poly(vinyl alcohol) (PVAL; $M_w = 500$; Kanto Chemical) were used as porogens without further purification.

Scheme 2

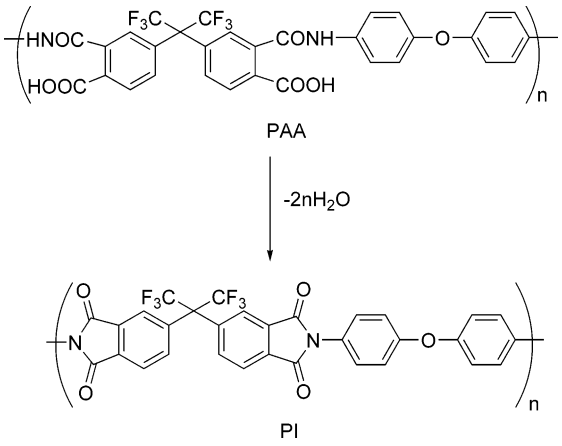

1-Methyl-2-pyrrolidinone (NMP; the good solvent), cyclohexane (the poor solvent), pyridine (the catalyst), and acetic anhydride (the dehydrating agent) were purchased from Wako Pure Chemical Industries and used without further purification.

A mixed NMP solution of PAA and porogen was prepared in the following manner. First, a given amount of an NMP solution of the porogen (1 wt %) was added to a diluted NMP solution of PAA. The final concentration of PAA was 1.5 wt %; the ratio of added porogen to the amount of PAA varied from 0.05 to 1.0 in the NMP solution.

In a typical reprecipitation method, a sample (100 μL) of the mixed NMP solution of PAA and porogen was injected via a microsyringe into vigorously stirred cyclohexane (10 mL) as the poor solvent at room temperature. The following two-step imidization[19] was performed to convert PAA to PI (Scheme 2). For chemical imidization, a mixture of pyridine and acetic anhydride (1:1 molar ratio, 100 μL) was injected into the dispersion of PAA nanoparticles. After 3 h, the chemically imidized PI nanoparticles were separated using a centrifuge, dried in vacuo, and then cured and thermally imidized at 270 °C for 1 h, resulting in a yellowish powder of PI nanoparticles.

Scanning electron microscopy (SEM) images were recorded using a JEOL JSM-6700F instrument operated at an acceleration voltage of 15 kV and an emission current of 10 μA. Several droplets of the resulting porous PI nanoparticle dispersion liquid were cast on a glass slide and air-dried at room temperature; the glass slide was fixed on the sample holder using double-faced carbon tape.

Transmission electron microscopy (TEM) images were recorded using a JEOL JEM-2010 instrument operated at an acceleration voltage of 200 kV. One droplet of the porous PI nanoparticle dispersion liquid was applied to a 150-mesh carbon-coated copper grid and air-dried at room temperature.

Thermogravimetric analysis (TGA) was undertaken using a Perkin-Elmer Pyris 1 TGA apparatus operated at a heating rate of 10 K/min under a nitrogen atmosphere (50 mL/min).

IR spectra were recorded using a ThermoNicolet AVATAR 360 FT−IR spectrometer. Powdered PI nanoparticles were ground with KBr to prepare the pellet samples.

Results and Discussion

We investigated the fabrication of porous PI nanoparticles using two different polymers as porogens. The first polymer evaluated as the porogen was PVAL. Although both PVAL

(11) Kasai, H.; Nalwa, H. S.; Okada, S.; Oikawa, H.; Nakanishi, H. *Handbook of Nanostructured Materials and Nanotechnology*; Nalwa, H. S., Ed.; Academic Press: San Diego, CA, 1999; Vol. 5: Organics, Polymers, and Biological Materials.
(12) Kasai, H.; Kamatani, H.; Yoshikawa, Y.; Okada, S.; Oikawa, H.; Matsuda, H.; Nakanishi, H. *Jpn. J. Appl. Phys.* **1996**, *35*, L221.
(13) Katagi, H.; Kasai, H.; Okada, S.; Oikawa, H.; Matsuda, H.; Nakanishi, H. *J. Macromol. Sci. Pure Appl. Chem.* **1997**, *A34*, 2013.
(14) Trau, M.; Saville, D. A.; Aksay, I. A. *Science* **1996**, *272*, 706.
(15) Van der Biest, O. O.; Vandeperre, L. J. *Annu. Rev. Mater. Sci.* **1999**, *29*, 327.
(16) Zhao, G.; Ishizaka, T.; Kasai, H.; Oikawa, H.; Nakanishi, H. *Mol. Cryst. Liq. Cryst.* **2007**, in press.
(17) Yabu, H.; Higuchi, T.; Shimomura, M. *Adv. Mater.* **2005**, *17*, 2062.
(18) Okubo, M.; Takekoh, R.; Suzuki, A. *Colloid Polym. Sci.* **2002**, *280*, 1057.
(19) Suzuki, M.; Kasai, H.; Miura H.; Okada, S.; Oikawa, H.; Nihira, T.; Fukuro, H.; Nakanishi, H. *Kobunshi Ronbunshu* **2002**, *59*, 637 (in Japanese).

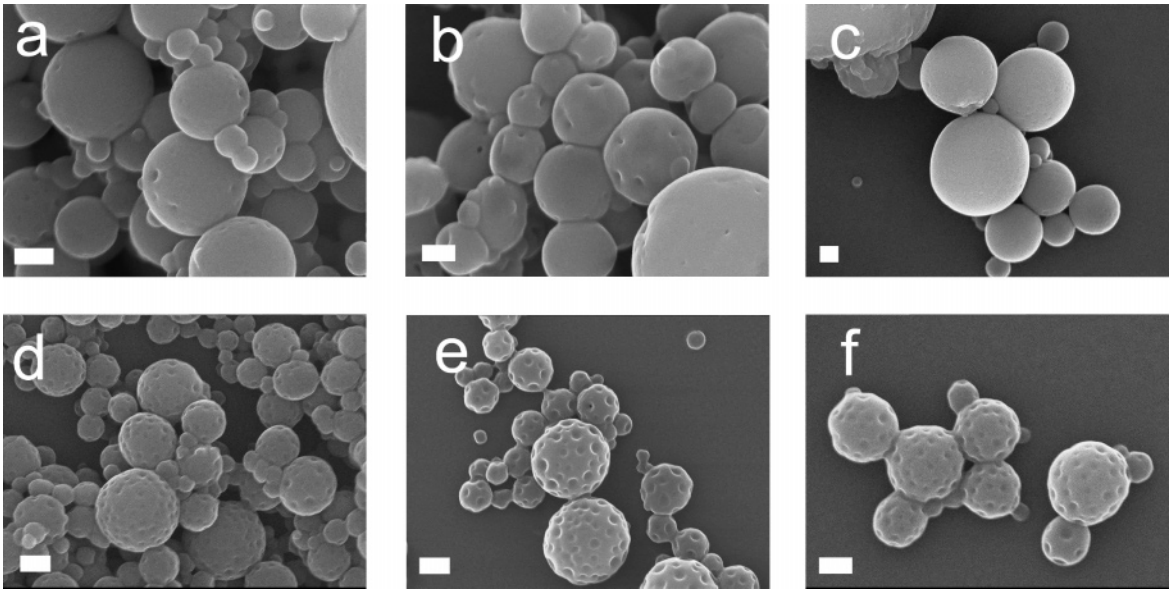

Figure 1. SEM images of porous PI nanoparticles prepared using various porogens at various contents: (a) PVAL (20 wt %), (b) PVAL (50 wt %), (c) PAS2 (20 wt %), (d) PAS1 (20 wt %), (e) PAS1 (40 wt %), and (f) PAS1 (60 wt %). The white scale bar represents a distance of 200 nm.

Table 1. Porous Morphologies of Various Samples

content of porogen	PVAL 50 wt %	PAS2 20 wt %	PAS1 40 wt %
pore number	few	none	many
pore size	30−50 nm		20−70 nm

and PAA dissolved in NMP, only some of the resulting PI nanoparticles possessed nanopores (images a and b of Figure 1). The fraction of porous PI nanoparticles was not, however, affected by the content of PVAL added. The second polymer evaluated as the porogen was PAS. Images c and d of Figure 1 indicate that the molecular weight of PAS clearly influenced the porous structure of the PI nanoparticles. Actually, the higher-molecular-weight PAS2 polymer did not provide any porous PI nanoparticles. In contrast, porous PI nanoparticles were successfully fabricated when using PAS1, as indicated in Figures 1d−f. The diameters of pores were in the range of 20−70 nm and the surface morphology remained almost constant when the PAS1 content was greater than 40 wt %. The results in Figure 1 are summarized in Table 1, which presents the effect of the porogen species on the resulting porous morphology of the PI nanoparticles.

Figure 2 exhibits SEM images of the porous PAA and/or PI nanoparticles at each stage of their fabrication. It is apparent that nanopores were already formed on the surface of the PAA nanoparticles prior to their imidization. In addition, the surface morphology was similar before and after performing the two-step imidization process.

The internal morphology of the porous PI nanoparticles displayed in Figure 1e was verified using TEM (Figure 3). We observe open-celled pores that lack interconnectivity only on the surface of the PI nanoparticles, i.e., no internal pores are visible within the PI nanoparticles. Nevertheless, it is difficult to confirm whether or not PAS remained inside these porous PI nanoparticles. Note that it would be necessary to eliminate residual PAS from the porous PI nanoparticles if they were to be used in device applications.

Figure 4 displays the results of TGA measurements. TGA curve i is that of ordinary PI nanoparticles that lack porous structures; they decomposed thermally at a temperature above 550 °C. On the other hand, PAS began to decompose at ca. 200 °C (TGA curve iv). The TGA curve ii is that of the chemically imidized porous PI nanoparticles, which also decomposed gradually at ca. 200 °C as a result of the removal of its residual PAS and solvents. The thermally imidized porous PI nanoparticles (TGA curve iii) yielded their 5% weight-loss temperature at 400 °C; they were thermally stable up to 300 °C, almost identical to the behavior of the ordinary PI nanoparticles (TGA curve i). This result suggests that almost no PAS remained within the thermally imidized porous PI nanoparticles.

Similar conclusions can be drawn from the IR spectra of the various nanoparticles Figure 5. Spectrum iv is that of PAS; its characteristic IR peaks appear at 1250 and 1170

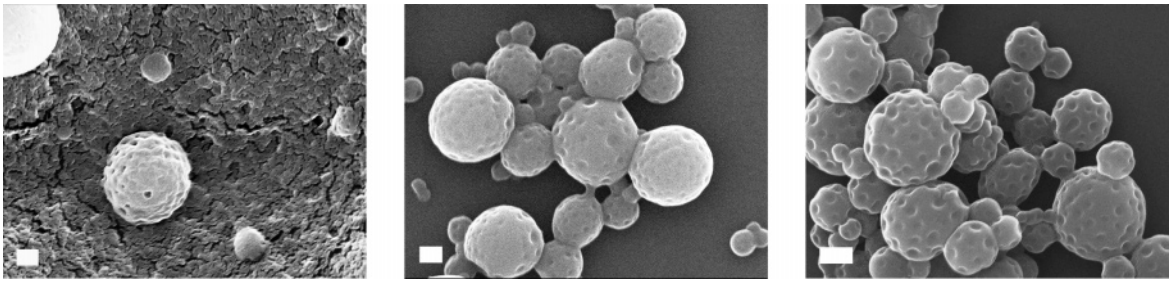

Figure 2. Morphologies of porous PAA and/or PI nanoparticles at each stage of fabrication: (left) immediately after injection; (middle) after chemical imidization; (right) after thermal imidization. Scale bars: 200 nm.

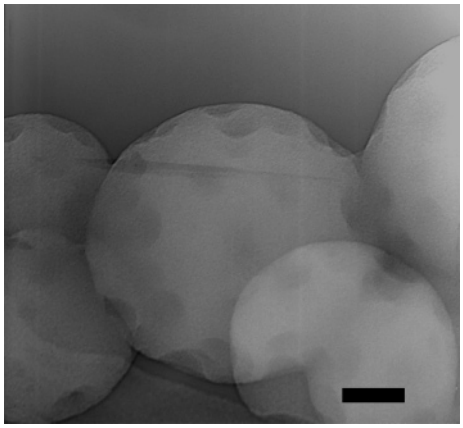

Figure 3. TEM image of the porous PI nanoparticles prepared from NMP solution of PAA and PAS1 (40 wt %; corresponding to Figure 1e). Scale bar: 50 nm.

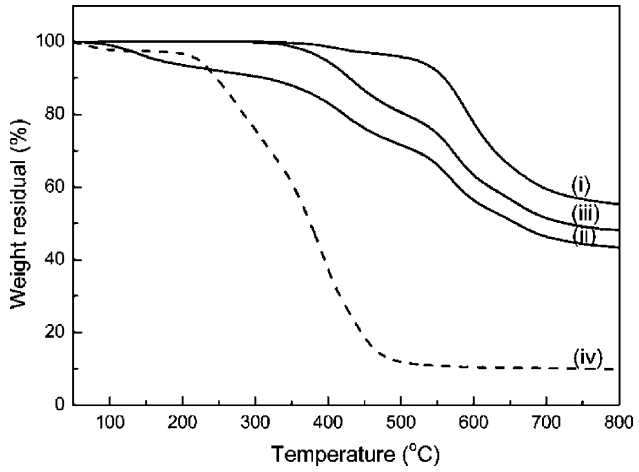

Figure 4. TGA (weight loss) curves recorded under N_2: (i) PI nanoparticles, (ii) chemically imidized porous PI nanoparticles, (iii) thermally imidized porous PI nanoparticles, and (iv) PAS1 (M_w = 2000). PAS1 (40 wt %) was added to samples ii and iii.

cm^{-1} (CO stretching). After thermal imidization, signals appeared at 1550 and 1380 cm^{-1}, corresponding to CNH and CN stretching vibrations, respectively (spectra ii and iii). The spectrum of the thermally imidized porous PI nanoparticles was virtually identical to that of the ordinary PI nanoparticles. This finding suggests that PAS was almost completely eliminated from the porous PI nanoparticles during thermal imidization, consistent with the results of TGA.

These findings have led us to propose a plausible mechanism of formation for the porous nanoparticles (Scheme 3). At first, fine droplets consisting of a mixture of NMP, PAA, and PAS1 were generated in cyclohexane immediately after injection. As the cyclohexane and NMP diffused into one another, PAA and PAS1 began to precipitate and microphase-separate in the surface layer of the fine droplets. According to the solubility parameters summarized in Table 2, cyclohexane is a much poorer solvent for PAS1 than for PAA. Thus, PAS1-rich microdomains formed in the surface layer. At this stage, the content of cyclohexane increased gradually within each fine droplet, with NMP remaining as the main component, but with a reduced solvent power. Thus, PAS1-rich microdomains formed within the fine droplets, because PAS1 is more soluble in NMP, as indicated in Table 2. Because these internal PAS1-rich microdomains did not possess such a clear interface, they might have then diffused toward the surface layer. Finally, the discontinuous and isolated PAS1-rich microdomains that formed in the surface layer were eliminated, leading to the formation of nanopores. Undoubtedly, the microphase separation leading to these porous surface nanostructure is a much more complicated process than this mechanism suggests; it must also depend on the molecular weight of PAS, the interfacial tension, the viscosity of the solvents, the mutual diffusion, and the compatibility between PAA and the porogen.

With regard to this mechanism, the selection of the porogen is very important aspect of the successful formation of the porous nanoparticles. A suitable porogen must be compatible with PAA to some extent; a suitable choice can be determined qualitatively by comparing the difference between the solubility parameters of PAA and the porogen.[21] The solubility parameter of PAS is closer to that of PAA

Scheme 3. Schematic Representation of the Mechanism of Formation of the Porous PI Nanoparticles.

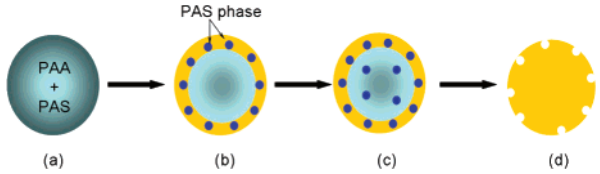

(a) A fine droplet of NMP, PAA, and PAS formed immediately after injection; (b, c) possible intermediate states, in which the yellow regions represent zones in which NMP and cyclohexane exchange through mutual diffusion processes; (d) the resulting porous PAA nanoparticle.

Table 2. Solubility Parameter[a] of the Materials Used in This Study

	PAA	cyclohexane	NMP	PVAL	PAS
solubility parameter (MPa$^{1/2}$)	20.8	16.8	23.1	30.5	23.6

[a] Solubility parameter was calculated using the Hoftyzer and Van Krevelen method.[20]

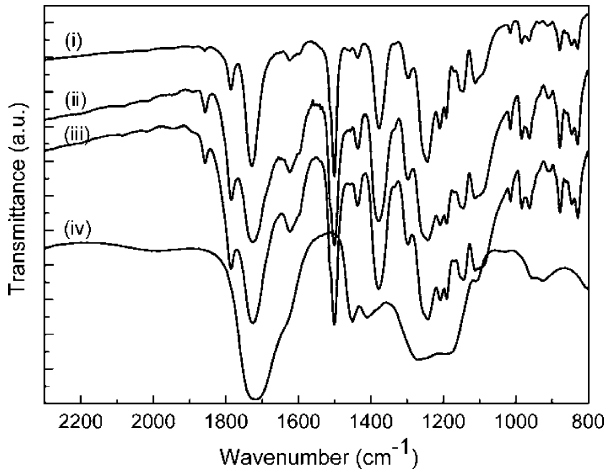

Figure 5. IR spectra recorded at each stage of imidization for porous PI nanoparticles prepared using various contents of PAS1. (i) PI nanoparticles; (ii) PAS1 (40 wt %) added and thermally imidized; (iii) PAS1 (80 wt %) added and thermally imidized; (iv) PAS1 (M_w = 2000).

(20) Krevelen, D. W. V. *Properties of Polymers*; Elsevier: Amsterdam, 1990.
(21) Coleman, M. M.; Serman, C. J.; Bhagwagar, D. E.; Painter, P. C. *Polymer* **1990**, *31*, 1187.

than it is to that of PVAL, which implies that PAS is more compatible with PAA. Certainly, hydrogen bonding between PAA and PAS must play a role in the formation of the porous PI nanoparticles. Therefore, we obtained better results when using PAS as the porogen (see Table 1 and Figure 1). On the other hand, the molecular weight of PAS had a great effect on the formation of pores within the PI nanoparticles; i.e., in NMP solution, an increase in the molecular weight of PAS may lower its compatibility with PAA and lead to nonporous structures being generated, as in the case for PAS2.

Conclusion

We fabricated porous PI nanoparticles using the reprecipitation method with PAS1 as the porogen. The sizes of the resulting PI nanoparticles were ca. 200−500 nm; their pores ranged in size from 20 to 70 nm. TGA and IR spectroscopic measurements indicated that almost no PAS1 remained in the porous PI nanoparticles after thermal imidization. TEM imaging suggested that the nanopores were superficial ones, rather than interconnected holes. These findings have led us to propose a mechanism accounting for the formation of the porous PI nanoparticles. We are currently investigating techniques for controlling the sizes of the porous PI nanoparticles, with the goal of using them to fabricate interlayer films exhibiting low dielectric constants.

Acknowledgment. The study was supported financially in part by the NEDO (New Energy and Industrial Technology Development Organization, Japan) Project. We thank Dr. A. Masuhara for technical suggestions regarding the TEM measurements. We are also grateful to Nissan Chemicals Industries for supplying us with poly(amic acid) (6FDA-ODA).

CM062709W